A numerical approach to the one-dimensional time-independent Schrödinger Equation

Sk Rahat Bin Salam

The University of Southern Mississippi,
School of Mathematics and Natural Sciences, Hattiesburg, Mississippi, 39406

E-mail: SkRahat.BinSalam@usm.edu

Abstract.

To solve the one-dimensional, time-independent Schrödinger equation numerically, the shooting method is employed. This second-order differential equation constitutes a boundary-value problem where physical solutions, or wave functions, exist only for a set of discrete eigenvalues or energies. The shooting algorithm transforms this to an initial value problem, the 4th order Runge-Kutta method is applied to integrate and Simpson's rule is used to normalize the wave functions. For the case of an infinite square well, the standard shooting method is carried out. A more refined technique, shooting to a midpoint, is adopted for symmetric potentials including the parabolic well and finite square well. This algorithm is further extended for quartic and delta-function potentials. In all cases, numerically demonstrated eigenvalues and eigenfunction are compared with the analytical solutions and show the accuracy of this computational approach.

1. Introduction

The principles of quantum mechanics govern the behavior of particles at the microscopic level [1]. The one-dimensional time-independent Schrödinger equation explains how the stationary states of these microscopic particles of mass m behave for a potential $V(x)$ [1]. The equation is expressed as:

$$-\frac{\hbar^2}{2m}\frac{d^2\psi(x)}{dx^2} + V(x)\psi(x) = E\psi(x) \tag{1}$$

Here, $\psi(x)$ is the wavefunction, $\hbar$ is the reduced Planck constant, which contains all the information about the state of the particle, and E is the total energy of that state. Rearranging gives

$$\frac{d^2\psi(x)}{dx^2} = -k^2\psi(x), \qquad k^2 = \frac{2m}{\hbar^2}(E - V(x)). \tag{2}$$

This is an eigenvalue equation where the solutions, or eigenfunction, only exist for a discrete set of energy eigenvalues E [2, 3]. These quantized energies differentiate quantum mechanics from the continuous energy spectrum in a classical mechanics. To

simplify the procedure, the Schrödinger equation is often expressed in dimensionless form:

$$\frac{d^2\psi(x)}{dx^2} = \gamma^2(v(x) - \epsilon)\psi(x), \tag{3}$$

where

$$\gamma^2 = \frac{2ma^2V_0}{\hbar^2}, \qquad V(x) = V_0 v(x), \qquad \epsilon = \frac{E}{V_0}. \tag{4}$$

This framework makes the calculation of eigenvalues and eigenfunction easier for different kind of potentials [4]. The parameter γ characterizes the "quantumness" of the system. For this dimensionless equation to be consistent, the variable x is typically understood to be rescaled by the characteristic length a. The solutions to this equation possess a definite parity, which sets the conditions required at the midpoint (chosen as $x = 0$):

- Even solutions must satisfy $\psi(-x) = \psi(x)$, which implies a zero slope at the center: $\psi'(0) = 0$.
- Odd solutions must satisfy $\psi(-x) = -\psi(x)$, which implies the wavefunction is zero at the center: $\psi(0) = 0$.

1.1. The Infinite Square Well

The infinite square well or a particle in a box is one of the simplest model in quantum mechanics. It describes a particle trapped between two impenetrable barriers. The potential $V(x)$ is defined as zero inside a region of length L and infinite everywhere else.

$$V(x) = \begin{cases} 0, & 0 < x < a, \\ \infty, & \text{otherwise.} \end{cases} \tag{5}$$

Inside the well, the equation reduces to

$$\frac{d^2\psi(x)}{dx^2} = -k^2\psi(x), \quad k^2 = \frac{2mE}{\hbar^2}. \tag{6}$$

Because the depth of the potential well is infinite, the particle cannot exist at or beyond the edges. This criterion sets the wavefunction to be zero at the boundary of the well.

$$\psi(0) = 0 \quad \text{and} \quad \psi(L) = 0 \tag{7}$$

It yields solutions

$$\psi_n(x) = A\sin\Big(\frac{n\pi x}{a}\Big), \quad n = 1, 2, 3, \ldots \tag{8}$$

with discrete energies

$$E_n = \frac{\hbar^2 n^2 \pi^2}{2ma^2}. \tag{9}$$

1.2. The Finite Square Well

The finite square well is a more realistic confined physical model where the potential barriers have a finite height, V_0. For kind of potential, the penetration depth is the distance outside the potential well where the probability significantly decreases. A famous and profound quantum phenomenon is observed because of this small change which is known as tunneling. For a well centered at the origin with width $2a$, the potential is:

$$V(x) = \begin{cases} -V_0, & |x| < a, \\ 0, & |x| \geq a. \end{cases} \tag{10}$$

For bound states ($E < 0$), the wavefunction is no longer forced to be zero at the walls. Instead, it decays exponentially into the edge of boundary region. The conditions require that both $\psi(x)$ and its derivative $\psi'(x)$ be continuous at the boundaries ($x = \pm a$) and that the wavefunction vanishes at infinity ($\psi(x) \to 0$ as $x \to \pm\infty$). For bound states, the solutions are oscillatory inside the well and exponential outside. Applying continuity conditions leads to transcendental equations:

$$\tan(ka) = \frac{\kappa}{k} \quad \text{(even states)}, \qquad \tan(ka) = -\frac{k}{\kappa} \quad \text{(odd states)}, \tag{11}$$

with

$$k = \frac{\sqrt{2m(E+V_0)}}{\hbar}, \quad \kappa = \frac{\sqrt{-2mE}}{\hbar}. \tag{12}$$

1.3. The Parabolic Well: The Quantum Harmonic Oscillator

One of the most important model system in all of physics is the quantum harmonic oscillator or the parabolic potential well [1]. It is used to approximate the behavior of systems near a point of stable equilibrium, like the vibration of atoms in a molecule. The potential energy increases quadratically with displacement from the origin:

$$V(x) = \frac{1}{2} m\omega^2 x^2 \tag{13}$$

To be physically realistic, the wavefunction must be normalizable, which means it must vanish at infinity.

$$\psi(x) \to 0 \quad \text{as} \quad x \to \pm\infty \tag{14}$$

The eigenfunctions are

$$\psi_n(x) = N_n \, e^{-\frac{m\omega x^2}{2\hbar}} \, H_n\left(\sqrt{\frac{m\omega}{\hbar}}\, x\right), \tag{15}$$

with Hermite polynomials H_n, and equally spaced energies

$$E_n = \hbar\omega \left(n + \frac{1}{2}\right). \tag{16}$$

1.4. Quartic Potential

The quartic potential is

$$V(x) = \alpha x^4. \tag{17}$$

No closed-form solutions exist, but numerical integration yields bound states with eigenfunctions of definite parity and energies that increase faster than linearly with n.

1.5. Delta-Function Potential

The delta-function potential is

$$V(x) = -\lambda\delta(x). \tag{18}$$

The wavefunction is continuous, but its derivative satisfies

$$\psi'(0^+) - \psi'(0^-) = -\frac{2m\lambda}{\hbar^2}\psi(0). \tag{19}$$

There is a single bound state:

$$\psi(x) = \sqrt{\kappa}\, e^{-\kappa|x|}, \quad \kappa = \frac{m\lambda}{\hbar^2}, \tag{20}$$

with bound-state energy

$$E = -\frac{m\lambda^2}{2\hbar^2}. \tag{21}$$

The Lippmann–Schwinger equation uses Green's functions to express the wavefunction in terms of the potential and free solutions. The time-independent Schrödinger equation can be written using the Green's function $G(x, x'; E)$:

$$(E - \hat{H})G(x, x'; E) = \delta(x - x'), \quad \hat{H} = -\frac{\hbar^2}{2m}\frac{d^2}{dx^2} + V(x).$$

The wavefunction satisfies

$$\psi(x) = \int G(x, x'; E)V(x')\psi(x')\, dx'.$$

For the free particle ($V = 0$), the Green's function is

$$G_0(x, x'; E) = -\frac{m}{\hbar^2\kappa}\, e^{-\kappa|x-x'|}, \quad \kappa = \frac{\sqrt{-2mE}}{\hbar}, \quad E < 0.$$

With $V(x) = -\lambda\delta(x)$, the Lippmann–Schwinger equation becomes

$$\psi(x) = -\lambda G_0(x, 0; E)\, \psi(0).$$

Self-consistency requires

$$1 + \lambda G_0(0, 0; E) = 0 \quad \Rightarrow \quad \kappa = \frac{m\lambda}{\hbar^2}.$$

Thus the bound state energy is

$$E = -\frac{m\lambda^2}{2\hbar^2}.$$

The δ-function potential supports exactly one bound state using the Green's function scheme.

2. Method

The central aim of this study is to numerically solve the one-dimensional time-independent Schrödinger equation by transforming the boundary-value problem into an initial-value problem. This allows the transformation to be handled using precise numerical framework. To achieve this, the shooting method, the shooting-to-midpoint refinement, the fourth-order Runge–Kutta (RK4) integration, Simpson's rule for normalization, and the bisection method for eigenvalue refinement are combined. Together, these techniques provide a consistent algorithm that can be applied to a variety of potentials.

2.1. Shooting Method

The Schrödinger equation is a second-order boundary-value problem. The shooting method transforms it into an initial-value problem by imposing trial boundary conditions at one end of the computational domain where the second one is a guess:

$$\psi(x_{\min}) = 0, \quad \psi'(x_{\min}) = 1. \tag{22}$$

The wavefunction is then propagated across the domain for a trial energy E where $x = L$. For arbitrary E, the solution fails to satisfy the boundary condition at the far end. Only for discrete eigenvalues does the solution satisfy both boundary conditions, yielding physically valid eigenfunctions [5].

2.2. Shooting-to-Midpoint Method

For symmetric potentials, efficiency is improved by integrating from both ends of the domain toward the midpoint $x = 0$ by propagaing from both the left ($x = -L$ and the right ($x = +L$)boundaries. The solutions are compared at the midpoint using the parity conditions which define the mismatch:

- Even states: $\psi'(0) = 0$,
- Odd states: $\psi(0) = 0$.

After observing the mismatch at $x = 0$, this method examines the trail energies. This approach simplifies the mismatch function and increases computational efficiency, while ensuring that eigenfunctions are continuous across the full interval $[-L, L]$. The bisection method refines the eigenvalue found from the change of sign in mismatch function.

2.3. Runge–Kutta Method (RK4)

Numerical propagation is performed using the classical fourth-order Runge–Kutta method. For an equation

$$\frac{dy}{dx} = f(x, y), \tag{23}$$

the RK4 scheme evaluates

$$\begin{aligned} k_1 &= h[f(x_n, y_n)] \\ k_2 &= h[f(x_n + \frac{h}{2}, y_n + \frac{k_1}{2})] \\ k_3 &= h[f(x_n + \frac{h}{2}, y_i + \frac{k_2}{2})] \\ k_4 &= h[f(x_n + h, y_n + k_3)] \end{aligned} \tag{24}$$

The global error is of order $\mathcal{O}(h^4)$, making this method highly suitable for oscillatory wavefunctions [4, 6].

2.4. Simpson's Rule for Normalization

Normalization of eigenfunctions requires

$$\int_{-\infty}^{\infty} |\psi(x)|^2 dx = 1. \tag{25}$$

On a uniform grid, this is approximated by the composite Simpson's rule:

$$I \approx \frac{h}{3}\Big[f(x_0) + 4\sum_{\text{odd}} f(x_i) + 2\sum_{\text{even}} f(x_i) + f(x_N)\Big]. \tag{26}$$

with $f(x) = |\psi(x)|^2$. The normalization constant is then applied to rescale $\psi(x)$.

2.5. Bisection Method

Eigenvalues are obtained by finding roots of the mismatch function $M(E)$. If $M(E)$ changes sign in $[E_a, E_b]$, then a root exists in the interval. The midpoint is

$$E_c = \frac{E_a + E_b}{2}. \tag{27}$$

The interval is updated depending on the sign of $M(E_c)$. Iteration continues until

$$|E_b - E_a| < \epsilon, \tag{28}$$

ensuring convergence to the eigenvalue within the specified tolerance.

3. Result

3.1. Infinite square well

The general behavior of wavefunction for the infinite square well is reflected in Figure 1. These solutions correspond to the ground state ($n = 1$), first excited state ($n = 2$), second excited state ($n = 3$), third excited state ($n = 4$) and fourth excited state ($n = 5$). At the boundaries of the well, the wavefunctions vanish in accordance with the analytical solutions. This reflects the impenetrability of the barriers in infinite square well.

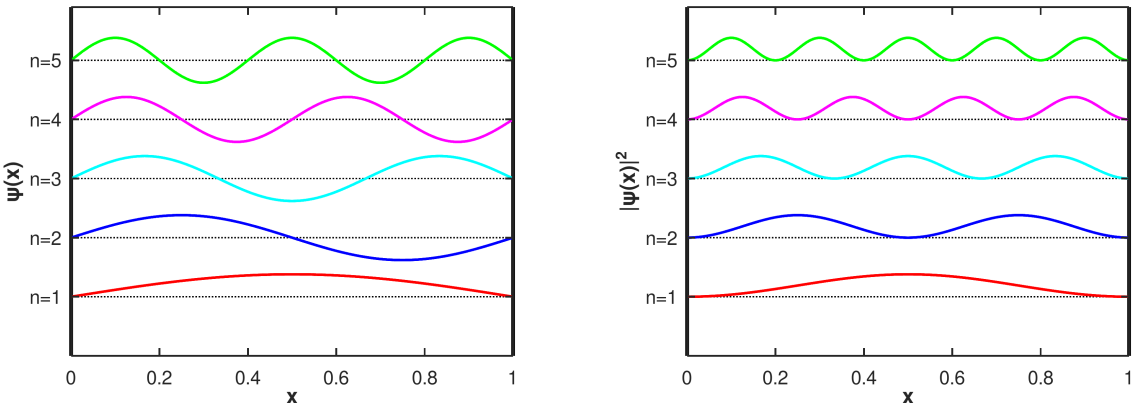

(a) $\psi(x)$ vs. x (b) $|\psi(x)|^2$ vs. x

Figure 1. Infinite square well results:(a) wavefunction $\psi(x)$ and (b) probability density $|\psi(x)|^2$. These are the first five eigenfunctions and probability density of a particle confined within an infinite square well. The solutions. The ground state ($n = 1$), 1st excited state ($n = 2$), 2nd excited state ($n = 3$), 3rd excited state ($n = 4$) and 4th excited state ($n = 5$) are denoted with red, blue, cyan, magenta and green lines respectively. The eigenfunctions diminish at the boundaryies which is displayed with bold black vertical lines exhibiting higher number of nodes with an increasing number of n. The probability density also follows the same pattern.

The $|\psi(x)|^2$ vs x graph also conforms to the analytic counterparts with sinusoidal oscillations with the number of nodes increasing with the energy levels. In Figure 2, the expected energy grew in quadratic fashion as per the theoretical values confirming the high accuracy of shooting method.

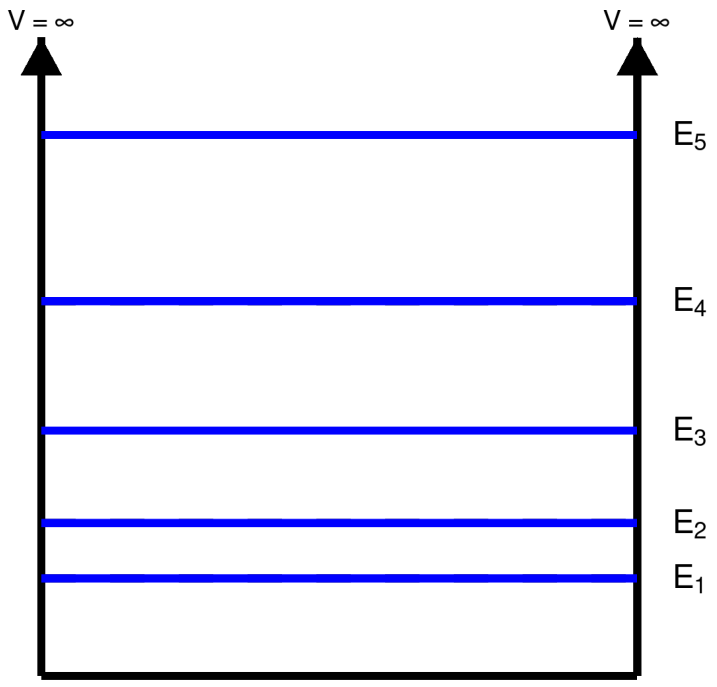

Figure 2. The eigenfunctions for ground state ($n = 1$), 1st excited state ($n = 2$), 2nd excited state ($n = 3$), 3rd excited state ($n = 4$) and 4th excited state ($n = 5$) are stacked on top of each other with blue lines portraying the gap between them in quadratic order.

3.2. Finite square well

In Figure 3, the confinement of a particle in a finite square well is presented with the eigenfunctions. Outside the boundary of the well, the wavefunctions are decaying exponentially while inside the well, these eigenfunctions are sinusoidal. This clearly represents the quantum tunneling phenomenon. The periodic nature of symmetric and antisymmetric nature is exhibited. The normalized wavefunctions also are in accordance with the analytical solutions.

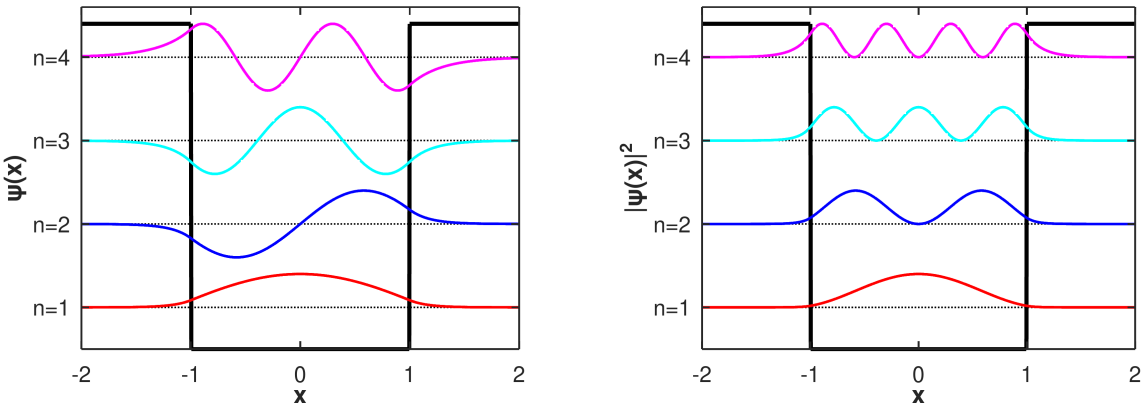

(a) Finite square well: $\psi(x)$ vs. x

(b) Finite square well: $|\psi(x)|^2$ vs. x

Figure 3. Finite square well results shown side-by-side: (a) wavefunction $\psi(x)$ and (b) probability density $|\psi(x)|^2$. These are the first five eigenfunctions and probability density of a particle confined within an infinite square well. The solutions. The ground state ($n = 1$), 1st excited state ($n = 2$), 2nd excited state ($n = 3$) and 3rd excited state ($n = 4$) are denoted with red, blue, cyan and magenta lines respectively. The eigenfunctions do not diminish at the boundaryies which is displayed with bold black vertical lines exhibiting higher number of nodes with an increasing number of n. The probability density also follow the same pattern.

3.3. Parabolic well

The wavefunctions for the parabolic well or quantum harmonic oscillator are shown in Figure 4. The confined potential is plotted as a bold black curve.

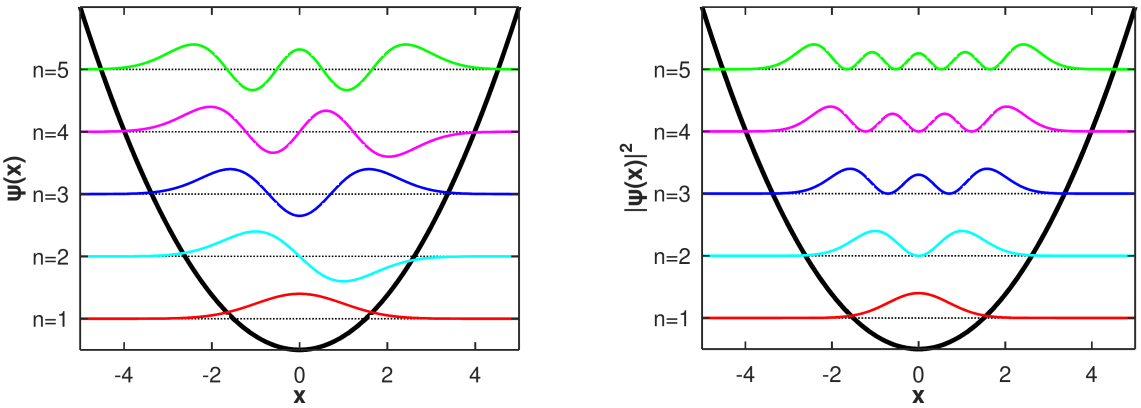

(a) Parabolic well well: $\psi(x)$ vs. x

(b) Parabolic well: $|\psi(x)|^2$ vs. x

Figure 4. Parabolic well results shown side-by-side: (a) wavefunction $\psi(x)$ vs x and (b) probability density $|\psi(x)|^2$. These are the first five eigenfunctions and probability density of a particle confined within an infinite square well. The solutions. The ground state ($n = 1$), 1st excited state ($n = 2$), 2nd excited state ($n = 3$), 3rd excited state ($n = 4$) and 4th excited state ($n = 5$) are denoted with red, cyan, blue, magenta and green lines respectively. The eigenfunctions diminish at the boundaryies which is displayed with bold black parabolic lines exhibiting higher number of nodes with an increasing number of n. The probability density also follow the same pattern.

The symmetry is seen in the ground state while the next states alternate between symmetry and anti-symmetry in parity. In here: antisymmetric for $n = 2$, symmetric for $n = 3$ and so on. In Figure 5, the energy eigenvalues are equally spaced where in the square wells, these were in contrast. The probability densities $|\psi(x)|^2$ is broadening with increasing energy states.

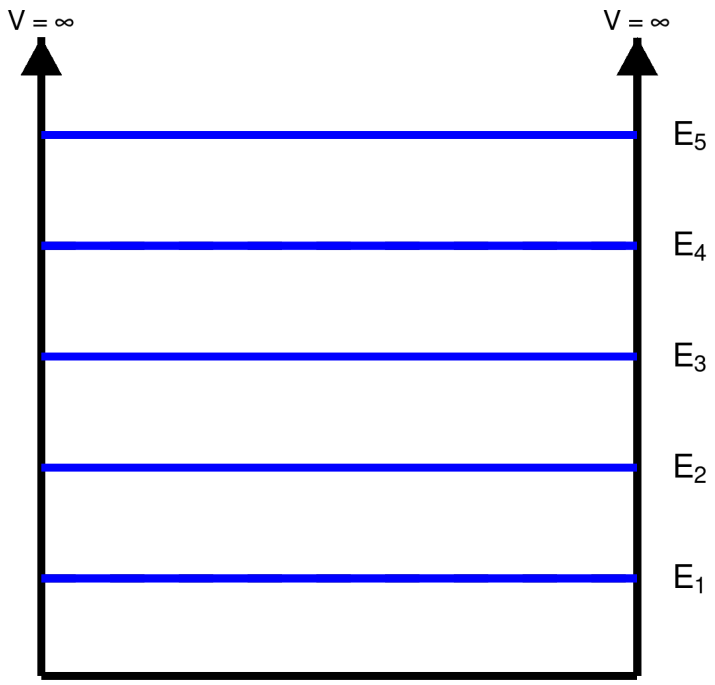

Figure 5. The eigenfunctions for ground state ($n = 1$), 1st excited state ($n = 2$), 2nd excited state ($n = 3$), 3rd excited state ($n = 4$) and 4th excited state ($n = 5$) are stacked on top of each other with blue lines portraying the equal gap between them.

3.4. Quartic potential

In Figure 6, eigenfunctions of the quartic potential, $V(x) = \alpha x^4$, are displayed. Compared to the parabolic potential, this produces more tightly confined wavefunctions close to origin. The eigenfunctions preserve parity symmetry by alternating even and odd states. Symmetry is observed in odd states whereas antisymmetry is displayed in the even states.

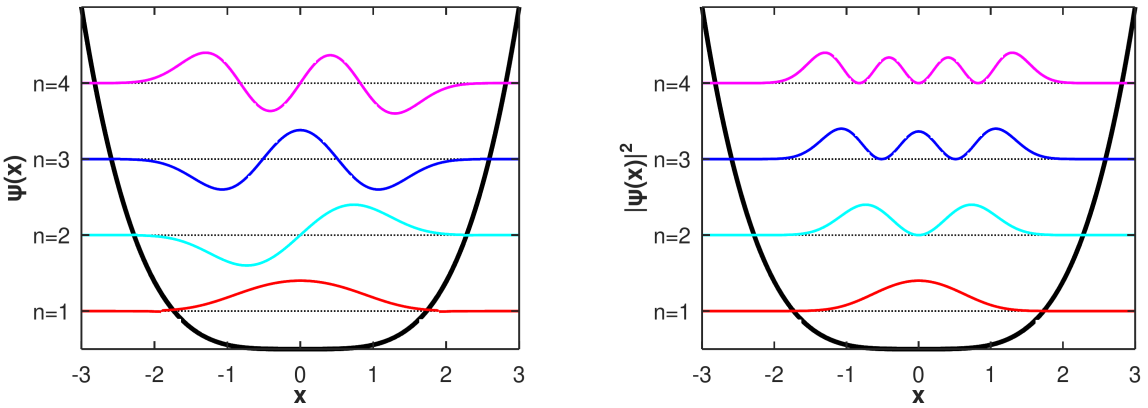

(a) Quartic well well: $\psi(x)$ vs. x (b) Quartic well: $|\psi(x)|^2$ vs. x

Figure 6. Quartic well results shown side-by-side: (a) wavefunction $\psi(x)$ vs x and (b) probability density $|\psi(x)|^2$. The ground state ($n = 1$), 1st excited state ($n = 2$), 2nd excited state ($n = 3$), 3rd excited state ($n = 4$) and 4th excited state ($n = 5$) are denoted with red, cyan, blue, magenta and green lines respectively.

3.5. Delta-function potential

The bound state wavefunction for delta function potential is presented in Figure 7. The potential is represented as a sharp localized well pointing downward at $x = 0$. This numerical solution displays an exponential decay in both direction from the origin and there will be only one eigenfunction with clear agreement with the theoretical expression.

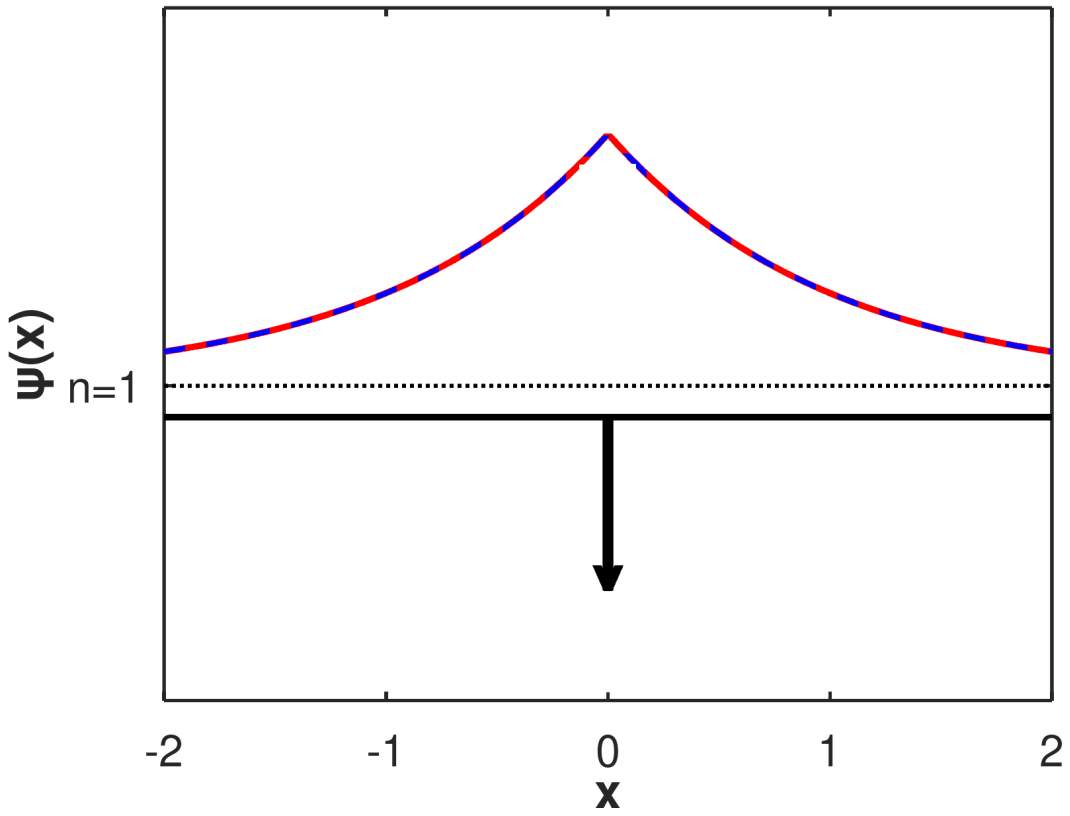

Figure 7. The bold black line with a pointer downward is displaying the delta-function potential. The wavefunction $\psi(x)$ is denoted by the red line and the blue dotted line where the red line is showing the numerical values and the blue dotted line is the analytical counterpart.

4. Conclusion

The shooting method was used at the beginning of the work for the infinite square well in one-dimensional time-independent Schrodinger equation and shooting-to-midpoint method was applied for other potentials. The fourth order Runge-Kutta method, Simpson's rule and bisection technique were utilized in this algorithm to numerically solve the problem. Parity-based boundary conditions were applied to certain potentials carefully. The algorithm reformulates boundary value problem into an initial value problem and successfully calculated the eigenvalues and eigenfunctions for different potentials.

For infinite square well, the method accurately reproduced the expected sinusoidal standing wave solutions with energy levels scaling proportional to the square of the number of the energy state. A different oscillatory behavior was seen in the finite square well near the edges of the boundaries showing nonzero probability in classically forbidden regions. In the parabolic potential well, the algorithm was consistent with the expected alternating parity and evenly spaced energy eigenvalues. For the quartic potential and

the delta function potential, the method captured the localized bound states. Exploring numerical schemes to solve Lippmann-Schwinger equation for arbitrary potentials using Green's functions can be a possible future work.

In all the cases, the numerically-obtained eigenvalues and eigenfunctions were consistent with the analytic solutions. The absolute error, calculated as the difference between the computed and theoretical values, was found to be consistently less than 10^{-14}. Beyond reproducing highly accurate results, this developed framework provides a reliable, precise approach for investigating wavefunctions and energy states for any arbitrary potential where analytical solutions are intractable.

[1] D. J. Griffiths, *Introduction to Quantum Mechanics*, 2 ed. (Pearson Prentice Hall, 2004).

[2] L. Lehtovaara, J. Toivanen, and J. Eloranta, "Solution of time-independent Schrödinger equation by the imaginary time propagation method," Journal of Computational Physics **221,** 148–157 (2007).

[3] R. Becerril, F. Guzmán, A. Rendón-Romero, and S. Valdez, "Solving the time-dependent Schrödinger equation using finite difference methods," Revista mexicana de física E **54,** 120–132 (2008).

[4] S. E. Koonin and D. C. Meredith, *Computational Physics (Fortran Version)* (Westview Press, 1990).

[5] D. Indjin, G. Todorović, V. Milanović, and Z. Ikonić, "On numerical solution of the Schrödinger equation: the shooting method revisited," Computer Physics Communications **90,** 87–94 (1995).

[6] W. Press, S. Teukolsky, W. Vetterling, and B. Flannery, *Numerical Recipes in Fortran 77 (2nd ed.)* (Cambridge University Press, 1992).